02

Effect of boundary conditions on reconstruction of absorption and scattering spectra in diffuse spectroscopy of skin: *in silicoo* study

© E.A. Sergeeva, D.A. Kurakina, A.A. Getmanskaya, M.Yu. Kirillin

Federal Research Center Gaponov-Grekhov Institute of Applied Physics
of the Russian Academy of Sciences (IPF RSA),
Nizhny Novgorod, Russia

e-mail: sergeeva_ea@ipfran.ru

Received July 02, 2025
Revised July 20, 2025
Accepted November 25, 2025

This study analyzes the feasibility of recovering skin spectral characteristics from optical diffusion spectroscopy data using an analytical model. The model accounts for a semi-infinite medium geometry, a limited detector aperture, and the presence of a refractive index mismatch at the medium boundary.

The employed approach involves two key stages. First, the spectral dependencies of the diffusion parameters the effective attenuation coefficient and the transport mean free path are recovered. Subsequently, the spectra of the absorption coefficient and the transport scattering coefficient are reconstructed from these parameters.

The accuracy of recovering the spectral characteristics of homogeneous dermis is compared for two scenarios: a contact probe (external refractive index $n_{out} = 1.5$) and a non-contact probe ($n_{out} = 1$). The analysis is performed for various levels of blood volume content and different sets of source–detector distances (1.8, 2.8, 3.8, and 4.8 mm).

The results show that the highest recovery accuracy (deviation not exceeding 10%) for both absorption and scattering spectra is achieved using the nearest three detectors in conjunction with contact probing. For non-contact registration using the same set of detectors, inaccuracies in recovering the transport mean free path in the near-infrared region lead to an overestimation of the absorption coefficient in this spectral range by up to 50%.

Furthermore, the effect of a superficial layer (epidermis) on the recovery of the underlying layer's (dermis) spectral characteristics is analyzed. The presence of the epidermis has practically no impact on the accuracy of recovering dermis parameters when using contact probing. In contrast, the use of a non-contact probing leads to a systematic underestimation of the absorption coefficient and a systematic overestimation of the scattering coefficient.

Keywords: diffuse reflectance spectroscopy, analytical model, Monte Carlo simulations.

DOI: 10.61011/EOS.2025.12.63177.44-25

1. Introduction

Optical diffuse spectroscopy (ODS) is widely used for non-invasive determination of the concentration of major chromophores in biological tissues, including skin, where the content of oxy- and deoxyhemoglobin, as well as melanin, is of interest. The ODS method is based on the registration of backscattering spectra in the wavelength range of 450–1100 nm using a set of sources and detectors located on or above the surface of the biological tissue, followed by the use of inverse problem algorithms. The principles of ODS are actively used in modern wearable medical and commercial devices where photoplethysmography at multiple wavelengths is applied to measure heart rate, blood oxygen saturation, and other physiological parameters. Modern ODS research systems allow to collect spatially-resolved data by detecting the signals using a linear array or matrix of contact fiber detectors coupled to a spectrometer (classical optical diffusion spectroscopy [1]) or using contactless hyperspectral cameras (optical diffusion imaging [2]). Data processing to restore the medium characteristics requires removal of the effect of instrumental parameters of the registration system, which is achieved through normalizing the signals or using calibration objects or using ratiometric measurements, when the signal for a specific pair „source–detector" is selected as a reference. Compensation of the system's instrumental characteristics is most successfully implemented using the „self-calibrated measurement" method, which requires a symmetrical arrangement of sources and detectors [3]. Another benefit of this measurement scheme is the shift of the sensitivity region from the boundary of the medium towards the interior, which reduces the contribution of surface structures to the signal spectra.

ODS applied in the quantitative assessment of chromophore content and its evolutional changes involves the use of analytical models that allow the parameters of biological tissues to be reconstructed from the measured optical signals. In biophotonics, biological tissues are characterized by absorption and scattering spectra. Various models of light propagation in randomly heterogeneous media are commonly used to calculate optical signals transmitted through biological tissue [4], but some methods may use empirical calibration curves [5]. In transmittance mode, when the

source and detector are located at opposite boundaries of the biotissue layer, a modified Lambert–Bouguer–Beer law is typically used [6], which is not suitable for diffuse reflection measurements in a wide spectral range. For ODS configuration the solution of the radiation transfer equation in the diffusion approximation for an infinite medium is widely used due to its simplicity [7]. To improve the accuracy of this approach, further modifications of this model have been proposed that take into account boundary conditions, such as geometry of a semi-infinite medium [8], discontinuity of the refractive index at the boundary of the medium [9], and limited numerical aperture of the detector [10]. The consideration of a small numerical aperture leads to different results of models [9,10] when calculating the ODS signals in fiber-optical skin diagnostics systems, where distances between the source and the detector do not exceed 5 mm [11].

These analytical models consider the skin as a medium with a uniform distribution of optical properties, while morphologically the skin consists of two layers — the epidermis and the dermis — with significantly different optical characteristics [12,13]. Thickness of the top layer — the epidermis which is also often considered to incorporate the corneous layer — in different skin areas makes from 50 to 500 μm [14]. As a rule, areas of so-called thin skin are of interest for research, where the thickness of the weakly absorbing corneous layer does not exceed 20 μm, and the epidermis has a thickness within 150 μm [15,16]. The epidermis contains melanin, while blood vessels are located in the deeper layer, the dermis, indicating an uneven distribution of chromophores in the skin. The scattering properties of these layers also vary significantly. In these conditions, it can be expected that the reconstructed characteristics of the biological tissue will be a complex combination of the characteristics of individual layers, making it difficult to quantify the content of individual chromophores. Nevertheless, modeling the most probable photon trajectories for the source-detector distances of a few millimeters shows that the measurement area has a well-known „banana-shaped“ structure, the central part of which lies mostly within the dermis. Therefore, it can be assumed that the effect of the epidermis is not so significant. The use of „self-calibration measurements“ also can result in lower effect of epidermis and the reconstructed skin parameters reflecting the dermis optical properties. However, in [10], it is demonstrated that when the skin surface contacts with air, the presence of the epidermis manifests itself in the form of an underestimated absorption coefficient and an overestimated transport scattering coefficient of the dermis. This effect was explained by the significant contribution of total internal reflection of radiation from the interface „tissue–air“ into the epidermal layer of the biological tissue. This configuration is typical for separate contact fibers between the source and detector, as well as for non-contact detection of signals by a hyperspectral camera with a small field of view. At the same time, for contact multichannel probes that completely cover the research area with their end surface, total internal reflection from the interface is not realized, since the refractive index of the probe body is close to 1.5, while the refractive index of biological tissues is about 1.4 [17]. According to the authors, the effect of the heterogeneous skin structure on the reconstructed spectra of optical characteristics from the ODS signals for a contact probe has not been studied.

The Monte Carlo numerical method for modeling radiation propagation in a scattering and absorbing medium is the gold standard for studying the formation of ODS signals for complex realistic medium geometry and system [5,18–20]. In this study, using Monte Carlo modeling, the effect of the epidermal layer and boundary conditions on the spectra of signals recorded by a fiber-optic system with a source-detector distance of 5 mm and a small numerical aperture of the detector is analyzed. This paper outlines the options for recording the ODS signal using contact and non-contact methods. Using the analytical model of ODS signals developed by the authors, which is applicable for these configurations, the authors performed a separate reconstruction of the absorption and transport scattering spectra of the skin for a single-layer medium that simulates the dermis and a double-layer medium mimicking the realistic skin structure. The effect of the epidermis and boundary conditions on the restored optical characteristics of the skin has been studied.

2. Materials and methods

The paper considers two options of the skin model: 1) a homogeneous semi-infinite medium with optical properties corresponding to dermis, 2) a double-layer plane-layered medium with optical properties of the top layer corresponding to epidermis and that of the bottom layer — to dermis. The top layer has thickness of 100 μm, which corresponds to the thickness of epidermis of a thin human skin [16]. The study was performed for two levels of blood content in the dermis: bloodless tissue, for which the volume content of blood in the tissue is $C_b = 0$, and blood-filled dermis with $C_b = 1\%$ [21]. The level of blood saturation with oxygen was taken $SiO_2 = 95\%$. The spectra of transport scattering coefficients $\mu_s'(\lambda)$ and absorption coefficients $\mu_a(\lambda)$ for the epidermis and the considered dermis variants, adapted from literature data [12,13], are presented in Fig. 1, *a,b*. The refractive index of both layers of biological tissue is chosen to be the same and equal to $n_t = 1.4$. The double-layer model instead of a more complex multi-layer model used previously for reconstructing the skin parameters in non-contact hyperspectral sensing [22] was selected, firstly, due to the fact that this study aims to reconstruct the optical characteristics of the tissue at each wavelength rather than the clinically relevant parameters of the biological tissue from the complete spectral data, and secondly, due to the fact that the concept of two vascular plexuses used in the multi-layer model does not always correspond to the data

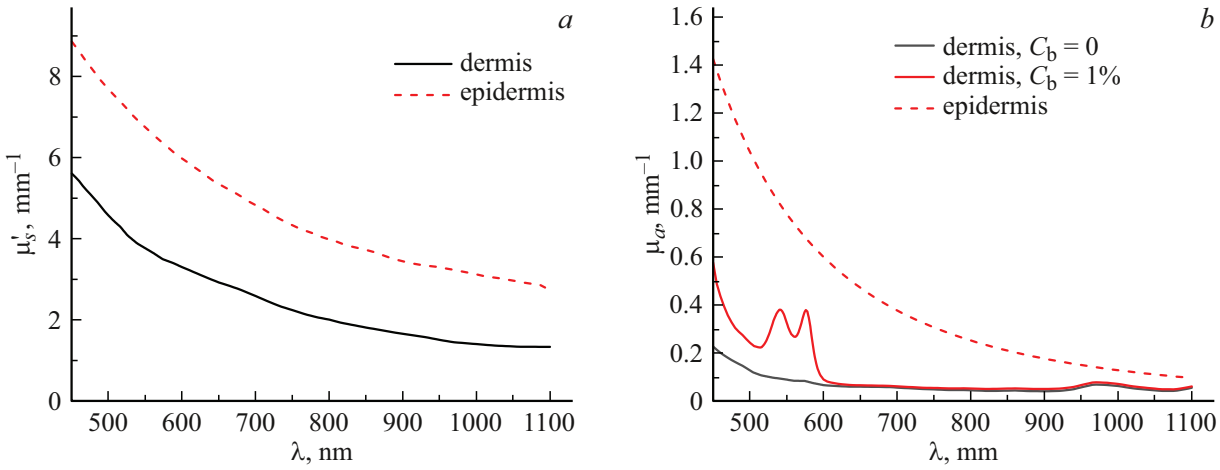

Figure 1. Spectra of transport scattering coefficient (a) and absorption coefficient (b) of epidermis and dermis for various blood-content levels C_{blood}.

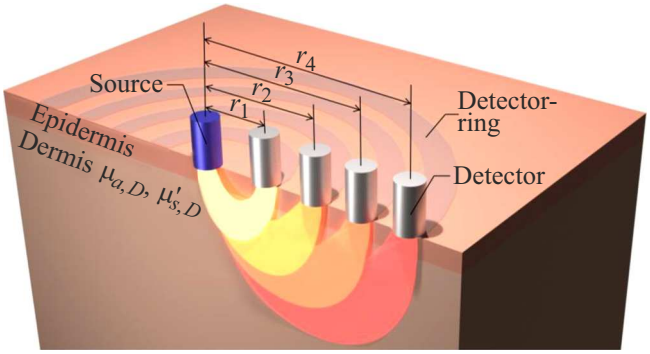

Figure 2. Sounding in ODS system ($r_{1,2,3,4} = 1.8$, 2.8, 3.8 and 4.8 mm).

on the distribution of hemoglobin concentration in the tissue volume [23].

The ODS signals were simulated using Monte Carlo method and a previously developed algorithm applied in previous works [10,11,20]. The algorithm's software is written in C++ language and is optimized for multi-core processors, allowing for parallelized calculations. In our study, we simulate the formation of ODS signals by a multichannel fiber-optic system similar to the one developed at the Institute of Applied Physics of the Russian Academy of Sciences [24]. The sounding scheme used in the simulated ODS system is presented in Fig. 2. The radiation is emitted in a point-like unidirectional beam perpendicular to the surface of the medium. The backscattered diffuse signal is detected using a line of fiber detectors, each characterized by a tip diameter of $d = 100\,\mu$m and a numerical aperture of $NA = 0.3$. The detector centers are located along a single straight line at distances $r_i = 1.8$, 2.8, 3.8, and 4.8 mm from the center of the emitting beam ($i = 1 \ldots 4$). To reduce the modeling noise, which has a significant impact at low detector numerical aperture, photons were detected within rings with radii corresponding to r_i and thicknesses equal to d (Fig. 2), followed by normalization to the ring area $S_i = 2\pi r_i d$. Modelling was made within the wavelength range 450–1100 nm with a 5 nm step, and in the wavelength interval 500–600 nm, where the most intensive blood absorption is observed the modelling step was 1 nm. $N = 5 \cdot 10^9$ was the amount of photons used in modelling.

In our previous study, we showed that the use of the radiometric method in ODS allows us to rule out the effect of instrument factors, including when using the self-calibration approach [24]. Therefore, in this work, we analyze the signal ratio spectra at various source–detector distances, and we also evaluate the accuracy of the optical properties of the medium based on such measurements.

One of the objectives of this research is to study the effect of boundary conditions on reconstruction of optical properties. To do this, the study considers two variants of outer environment characterized by the refractive index n_{out}:

— the refractive index of the outer environment is equal to $n_{\text{out}} = 1.5$, which simulates the skin examination using a contact probe with implemented fiber sources and detectors;

— the refractive index of outer medium is equal to $n_{\text{out}} = 1$, which simulates non-contact sounding through the air medium, for example, using a hyperspectral camera.

The modeling results include signal spectra $R_{\text{MC}}(r_j, \lambda)$ for all considered skin models, distances r_i, and two boundary condition options.

To reconstruct the optical properties an analytical model of the ODS signal based on RTE solution for a semi-infinite medium in the diffusion approximation was used, taking into account the boundary conditions and the small solid angle of detection, as described in the previous study [10]. This model is based on the following expression for the backscattered diffuse signal detected by a small-angle detector Ω_{det} from a homogeneous semi-infinite medium, as

a function of the transverse source–detector distance r:

$$R_{\mathrm{RM}}(r) = \frac{3T_{F0}}{4\pi l_t}\,\frac{\Omega_{\mathrm{det}}}{4\pi}\left[\frac{\exp(-\mu_{\mathrm{ef}} r)}{r} - \frac{\exp\left(-\mu_{\mathrm{ef}}\sqrt{r^2 + 4l_t^2(1+2m/3)^2}\right)}{\sqrt{r^2 + 4l_t^2(1+2m/3)^2}}\right]. \quad (1)$$

Here, the medium parameters are the derived characteristics — the effective diffuse attenuation coefficient $\mu_{\mathrm{ef}} = \sqrt{3\mu_a(\mu_a + \mu_s')}$ and the transport length $l_t = (\mu_a + \mu_s')^{-1}$. The value $T_{F0} = (4n_t n_{\mathrm{out}})/(n_t + n_{\mathrm{out}})^2$ is itself a Fresnel transmittance coefficient at normal light incidence. The parameter m describes the effect of interface on the magnitude of the diffuse field in the biotissue and is determined by the relative refractive index n_t/n_{out} [9]. For contact registration of ODS signals $n_{\mathrm{out}} = 1.5$ and $m = 1.03$, and for contactless registration through air $n_{\mathrm{out}} = 1$ and $m = 2.82$.

To recover the spectra of the parameters $\mu_{\mathrm{ef}}(\lambda)$ and $l_t(\lambda)$ using a radiometric approach, two spectrum ratios are formed at the wavelength λ:

$$\mathrm{Ratio}_{i,j} = R_{\mathrm{RM}}(r_i)/R_{\mathrm{RM}}(r_j)$$

and

$$\mathrm{Ratio}_{i,k} = R_{\mathrm{RM}}(r_i)/R_{\mathrm{RM}}(r_k),$$

$i \neq j \neq k$. The formed ratios depend only on the characteristics of the biological tissue at a given wavelength and the source–detector distance. Similar ratios shall also be formed for $R_{\mathrm{MC}}(r_j, \lambda)$ signals obtained using Monte Carlo simulation. $\mu_{\mathrm{ef}}(\lambda)$ and $l_t(\lambda)$ were reconstructed in Mathcad 14.0 by a concerted search of residuals minima relative to parameters μ_{ef}, l_t at each wavelength using Levenberg–Marquardt algorithm:

$$\begin{cases} \left|\dfrac{R_{\mathrm{RM}}(\mu_{\mathrm{ef}}, l_t, r_i)}{R_{\mathrm{RM}}(\mu_{\mathrm{ef}}, l_t, r_j)} - \dfrac{R_{\mathrm{MC}}(r_i, \lambda)}{R_{\mathrm{MC}}(r_j, \lambda)}\right| \xrightarrow[\mu_{\mathrm{ef}}, l_t]{} \min, \\ \left|\dfrac{R_{\mathrm{RM}}(\mu_{\mathrm{ef}}, l_t, r_i)}{R_{\mathrm{RM}}(\mu_{\mathrm{ef}}, l_t, r_k)} - \dfrac{R_{\mathrm{MC}}(r_i, \lambda)}{R_{\mathrm{MC}}(r_k, \lambda)}\right| \xrightarrow[\mu_{\mathrm{ef}}, l_t]{} \min. \end{cases} \quad (2)$$

The primary optical properties of the medium are calculated from the recovered parameters using the following formulas:

$$\mu_a = \mu_{\mathrm{ef}}^2 l_t/3, \quad (3a)$$

$$\mu_s' = \frac{1}{l_t} - \mu_a. \quad (3b)$$

The inverse problem was solved for two sets of distances (r_i, r_j, r_k): the near triple $(r_i, r_j, r_k) = (r_1, r_2, r_3)$ and the distant triple $(r_i, r_j, r_k) = (r_2, r_3, r_4)$. Earlier, in [20], it was shown that the distance between the source and the detector determines the depth of sounding, and the result of the reconstruction of optical properties may depend on the choice of distances. Therefore, the sets of distances were selected that provide the closest sounding depths, minimizing the effect of heterogeneity of optical properties distribution within the medium in real measurements. However, the model used for reconstruction of light propagation in biological tissue had to be valid for the selected distances. Previous works by the authors [10,11] also described this issue, and it was shown that the diffusion model (1) was in good agreement with the results of Monte Carlo simulations at $r > 2$ mm for the optical characteristics of the skin in a wide range of wavelengths. The distant triple of distances is better suited to this requirement. On the other hand, at the maximum distance, the signal–noise ratio should be acceptable for accurate reconstruction, which is more likely to be achieved for the near-range distances. Comparing the reconstruction results for different sets of source–detector distances will demonstrate the capabilities and limitations of the method in the specified range of values r.

3. Results and discussion

3.1. Characteristic spectra of ODS signals

As part of the study, the ODS signals were simulated using Monte Carlo method for both a homogeneous medium that simulates the dermis and a double-layer medium that simulates the layered structure of the epidermis + dermis. The simulation takes into account the difference in the optical properties of epidermis and dermis. Fig. 3 illustrates the ratios of spectra of ODS signals $\mathrm{Ratio}_{12} = R_{\mathrm{MC}}(r_1, \lambda)/R_{\mathrm{MC}}(r_2, \lambda)$ and $\mathrm{Ratio}_{24} = R_{\mathrm{MC}}(r_2, \lambda)/R_{\mathrm{MC}}(r_4, \lambda)$ for detectors with $r_1 = 1.8$ mm, $r_2 = 2.8$ mm and $r_4 = 4.8$ mm for the cases of contact probe ($n_{\mathrm{out}} = 1.5$) and contactless probe ($n_{\mathrm{out}} = 1$) for a bloodless dermis and a dermis with a 1% blood-content. It can be seen that in all cases, the signal ratio is lower for the non-contact probe, which is due to the influence of total internal reflection. As shown earlier in [25], the presence of total internal reflection leads to the concentration of scattered light under the surface, since the fraction of diffusely scattered photons that cannot leave the medium is quite large. This results in lower amount of photons emanating from the medium. Additionally, the diffuse flux reflected from the surface is itself an additional secondary source, which leads to a higher signal at greater distances and lower difference between the signals measured at two different distances. Thus, a configuration with non-contact detection of ODS signals leads to a lower signal level and potentially greater error in determining the optical properties of the medium.

The effect of enhancing the near-surface field can be shown using an analytical solution for the one-dimensional distribution of irradiance $\Phi_{\mathrm{dif}}(z)$ over depth z in the diffusion approximation for a wide-beam illumination, taking into account the quasi-directional component [26] and the

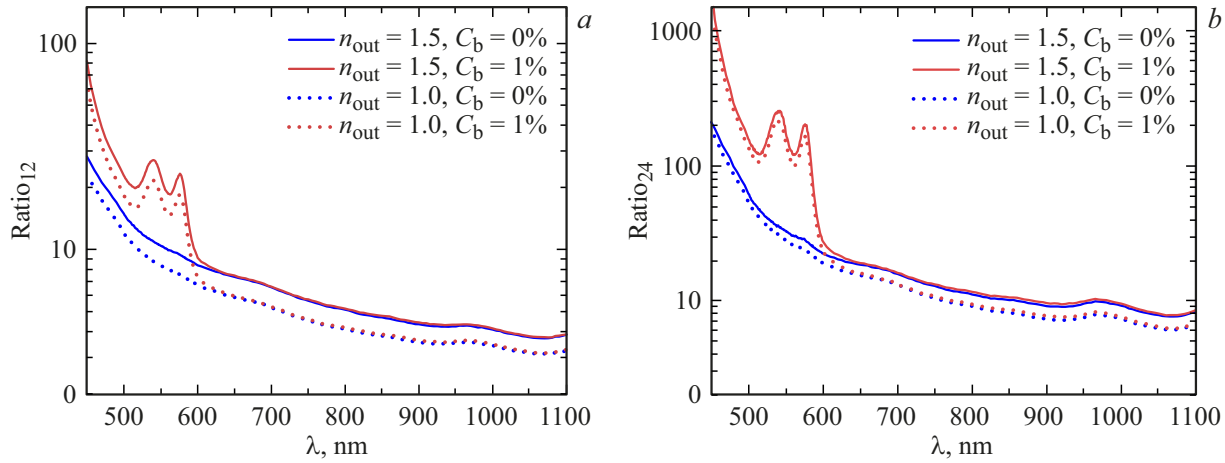

Figure 3. Ratios of ODS signals spectra $Ratio_{12}$ (a) and $Ratio_{24}$ (b) for homogeneous dermis with various degree of blood-content and outer environment with refractive indices $n_{out} = 1.5$ and $n_{out} = 1$.

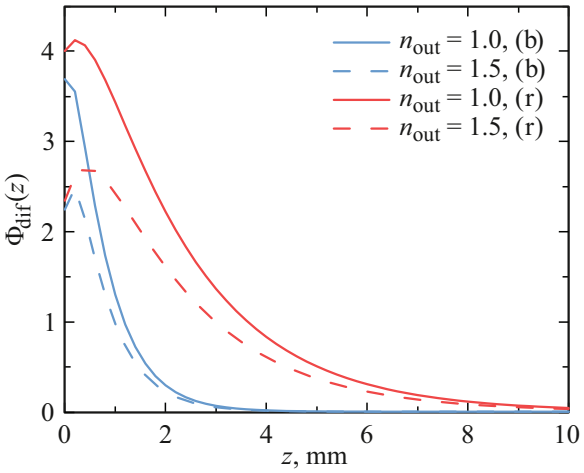

Figure 4. Uniform distribution of irradiance over the depth when illuminated by a wide beam, obtained in diffusion approximation accounting for the quasi-directional component and the refractive index jump for the optical properties typical for the blue („b“, $\mu_{ef} = 1.5\,\mathrm{mm}^{-1}$, $l_t = 0.2\,\mathrm{mm}$) and red („r“, $\mu_{ef} = 0.5\,\mathrm{mm}^{-1}$, $l_t = 0.5\,\mathrm{mm}$) wavelength range: solid curve $n_{out} = 1$, $m = 2.82$, dashed curve for $n_{out} = 1.5$, $m = 1.03$.

refractive index jump:

$$\Phi_{dif}(z) = \frac{3 - (\mu_{ef} l_t)^2}{1 - (\mu_{ef} l_t)^2}\,[1 + 2m/3]\,\frac{\exp(-\mu_{ef} z)}{1 + 2m\mu_{ef} l_t/3} - \frac{2}{1 - (\mu_{ef} l_t)^2}\exp(-z/l_t). \quad (4)$$

The dependence of irradiance on depth calculated using this formula for pairs of values μ_{ef}, l_t typical of the dermis in the blue and red ranges is shown in Figure 4 for two refractive indices of the outer environment. The irradiance for the case $n_{out} = 1$ (which corresponds to $m = 2.82$) exceeds that for the case $n_{out} = 1.5$ (which corresponds to $m = 1.03$) by a factor of 1.64 for the red range and by a factor of 1.71 for the blue range of wavelengths, which allows us to assess the role of total internal reflection in the formation of the diffuse field in biological tissue. The ratio between the diffuse reflection coefficient and the irradiance at the boundary for the one-dimensional case, obtained from the known boundary condition [27],

$$R_{dif} = \Phi_{dif}(z = 0)/2m \quad (5)$$

leads to a direct relationship between the diffuse reflection coefficient and the parameter m, which demonstrates a decrease in the reflected signal when there is total internal reflection:

$$R_{dif} = \frac{1 - (\mu_{ef} l_t)^{2/3}}{1 + \mu_{ef} l_t}\left[\frac{1}{1 + 2m\mu_{ef} l_t/3)}\right]. \quad (6)$$

Fig. 5 illustrates the effect of the epidermis on the ratio of $Ratio_{12} = R_{MC}(r_1, \lambda)/R_{MC}(r_2, \lambda)$ ODS signal spectra for different boundary conditions. Qualitatively, the dependencies resemble the signal ratio spectra for homogeneous dermis presented in Fig. 3, which indicates the dermis's crucial role in shaping backscatter signals and the possibility of reconstructing its optical properties. Earlier, in [10] for $n_{out} = 1$ it was demonstrated that ODS signals spectra themselves differed significantly for the homogeneous dermis and the double-layered medium with a surface absorbing layer (epidermis + dermis), however the ratio of ODS signals was a way less sensitive to the presence of epidermis. This effect was explained by the fact that a thin absorbing surface layer can be considered as a weakening filter, the effect of which can be represented as a declining spectrally dependent multiplicative factor (transmittance coefficient). As can be seen from Fig. 5, for contact detection ($n_{out} = 1.5$), when the role of total internal reflection is negligible, the effect of epidermis is maximally compensated when plotting the signals ratio, and $Ratio_{12}$ spectra for the single-layer and double-layer models are almost identical. For the non-contact detection ($n_{out} = 1$),

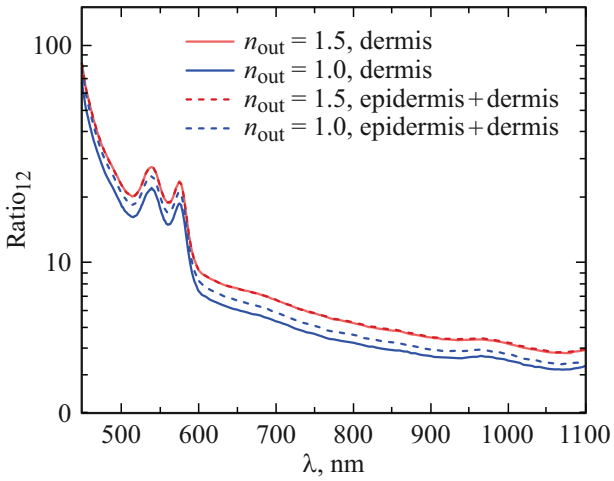

Figure 5. $\text{Ratio}_{12} = R_{MC}(r_1, \lambda)/R_{MC}(r_2, \lambda)$ of signals from two detectors for a dermis like single-layer medium and for a double-layer medium (epidermis+dermis) for different boundary conditions, compared: $n_{out} = 1$ and 1.5.

there is a slight difference in the values of Ratio_{12} ratios for homogeneous and double-layer skin models. When there's total internal reflection, the interaction of the near-surface diffuse field with the epidermis becomes more complex, which can have a systematic effect on the accuracy of dermis optical properties reconstruction.

3.2. Possible reconstruction of the spectra of optical properties of dermis from the ODS signals ratios

3.2.1. Single-layered skin model

Fig. 6 shows the results of reconstruction of the diffusion optical characteristics of dermis $\mu_{ef}(\lambda)$ and $l_t(\lambda)$ in a single-layer biotissue model using formulas (1) and (2) based on Monte Carlo modeling results. The graphs also show the spectra of the corresponding parameters $\mu_{ef,D}$ and $l_{t,D}$ for a homogeneous dermis, which were specified during the modeling process. The results are given for the bloodless dermis and dermis with a volumetric blood content of 1%, for the two sets of distances (r_1, r_2, r_3) and (r_2, r_3, r_4) and different boundary conditions ($n_{out} = 1.5$ and $n_{out} = 1$). From the presented graphs, it can be seen that the spectrum μ_{ef} is reconstructed with high accuracy and low noise levels for all the considered parameter options. A slightly lower value of μ_{ef} compared to $\mu_{ef,D}$ in visible area of the spectrum, most noticeable in the range of blood absorption peaks ($\lambda = 500-600$ nm), is apparently associated with a limited applicability of the diffusion approximation for the highly absorbing media. At the same time, the reconstructed spectra l_t are characterized by fluctuations of varying intensity, which leads to fluctuations in the absorption coefficient spectrum reconstructed using formula (3a). To eliminate the effect of fluctuations, the spectra $l_t(\lambda)$ are smoothed while maintaining the monotonicity of the resulting approximations, which are presented in the graphs. The lowest level of fluctuations is observed in the reconstructed spectrum $l_t(\lambda)$ for contact detection ($n_{out} = 1.5$) and the nearest triple of detectors (r_1, r_2, r_3). For this combination of parameters, the highest level of the detected ODS signal is achieved. For non-contact detection, the same three detectors show signal fluctuations in the spectral range 900−1100 nm, and the smoothed values l_t differ significantly from the specified values $l_{t,D}$. This effect is partly caused by the imperfections of the analytical model used to describe the ODS signal in the low absorption and scattering region, where the field is not completely diffuse and, in particular, does not conform to the imposed boundary condition [11]. If the most distant triple of detectors (r_2, r_3, r_4) is used to reconstruct the dermis parameters, then, the level of fluctuations in $l_t(\lambda)$ spectra rises for both boundary condition options due to a decrease in the signal level, but there is no any significant deviation of the smoothed values from the specified ones. This is an evidence of a better applicability of the analytical model used for reconstruction to the conditions of the ODS signal detection. It should also be noted that for all spectra recorded at distant sources, the level of fluctuations in the signals themselves is insignificant. These fluctuations are most pronounced in the range up to 500 nm, where the signal level is minimal due to the high absorption of the skin. The difference-based reconstruction scheme, which is based on signal ratios, makes the proposed method extremely sensitive to signal deviations and requires efforts to minimize all types of noise.

Results of reconstruction of the primary optical properties of homogeneous dermis $\mu_a(\lambda)$ and $\mu_s'(\lambda)$ obtained from the spectra μ_{ef} and l_t by formulas (3a) and (3b), respectively, are shown in Fig. 7. All the considered configurations are characterized by an underestimation of the absorption coefficient, accompanied by a slight overestimation of the transport scattering coefficient in the wavelength range 450−600 nm. This cross-talk error effect occurs due to an error in the definition of l_t (Fig. 6), which is further found in formulas (3). In cases where it is impossible to reconstruct the transport length, the cross-talk error effect significantly limits the separate reconstruction of the absorption and scattering spectra due to the uncertainty in their ratio, as they are included in the $\mu_{ef}(\lambda)$ spectrum as a product.

The highest accuracy of the absorption and scattering spectra reconstruction is provided for the near triple of detectors and contact detection for both values of the dermis blood-content (Fig. 7, *a*): the deviation from the corresponding set values $\mu_{a,D}$ and $\mu_{s,D}'$ does not exceed 10%. For the non-contact detection using the same detectors (Fig. 7, *b*), the error in reconstruction of l_t in the range 900−1100 nm leads to an overestimated absorption in this region by up to 50%. For the distant triple of detectors, the reconstruction error for scattering and absorption values is within 12% for both contact and non-contact detection methods (Figs. 7, *c* and 7, *d*). It should be noted that if a high signal-to-noise

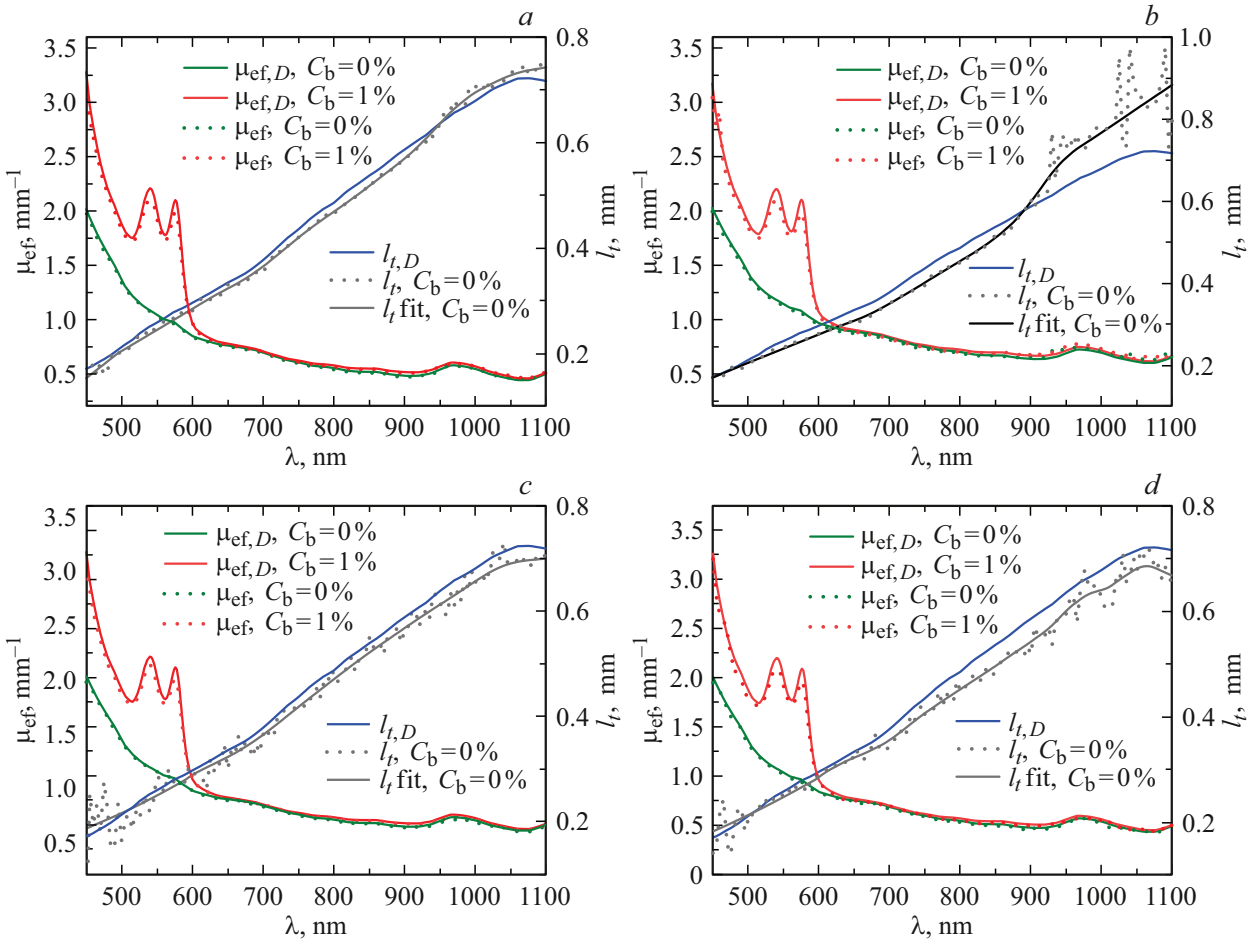

Figure 6. Spectra of diffusive optical characteristics μ_{ef} and l_t of a homogeneous dermis with blood-content $C_b = 0$ and $C_b = 1\%$ reconstructed from the ODS signals spectra obtained via modeling by Monte Carlo method for the near (*a,b*) and distant (*c,d*) triples of detectors, as well as for the contact (*a,c*) and contactless (*b,d*) signals registration. Points correspond to the reconstructed parameters, solid lines — to homogeneous dermis parameters ($\mu_{ef,D}$ and $l_{t,D}$) set during modeling, as well as to the smoothed reconstructed spectrum l_t (fit).

ratio can be achieved in a real experiment, the use of distant detectors for optical characterization is preferable due to the applicability of the analytical ODS signal model.

3.2.2. Double-layered skin model

The case of a double-layered medium is somewhat more complicated in terms of interpretation of the optical properties reconstructed according to algorithm (2), since dermis occupies the majority of the measuring volume; yet, the thin surface layer of epidermis is itself a way more scattering and absorbing and, thus, may influence the shape of the processed signals (Fig. 5). It has been previously shown [10] that for the case $n_{out} = 1$, the presence of the epidermis leads to overestimated reconstructed values of the transport scattering coefficient and underestimated values of the absorption coefficient, while the effective attenuation coefficient is insensitive to the presence of the epidermis and coincides with that of a homogeneous dermis.

Fig. 8 illustrates the results of reconstruction of diffusion optical characteristics of dermis $\mu_{ef}(\lambda)$ and $l_t(\lambda)$ in a double-layer model of biological tissue when the semi-infinite layer of dermis with set parameters $\mu_{ef,D}$ and $l_{t,D}$ is covered with a layer of epidermis with parameters $\mu_{ef,E}$ and $l_{t,E}$ and thickness of 100 μm. Note that the presence of epidermis has almost no effect on the reconstruction quality for μ_{ef} spectrum for all the configurations considered, and the reconstructed μ_{ef} values are similar to those for a homogeneous dermis. The reconstructed spectra l_t for the contact detection (Fig. 8, *a* and 8, *c*) also correspond to the spectra obtained for a homogeneous dermis (Fig. 6, *a* and 6, *c*). However, the values l_t for contactless detection (Fig. 8, *b* and 8, *d*) are significantly less than the specified ones and are characterized by a low level of fluctuations, i.e. they systematically lower than the true values. The discrepancy ranges from 5% to 40% and shows different behavior for the near (Fig. 8, *b*) and distant (Fig. 8, *d*) triplets of detectors. This systematic discrepancy appears to be related to the multiple passage of photons reflected from the photons boundary through the epidermal layer, the spectrum $l_{t,E}(\lambda)$ of which is also shown in the graphs. In the blue-green region of the

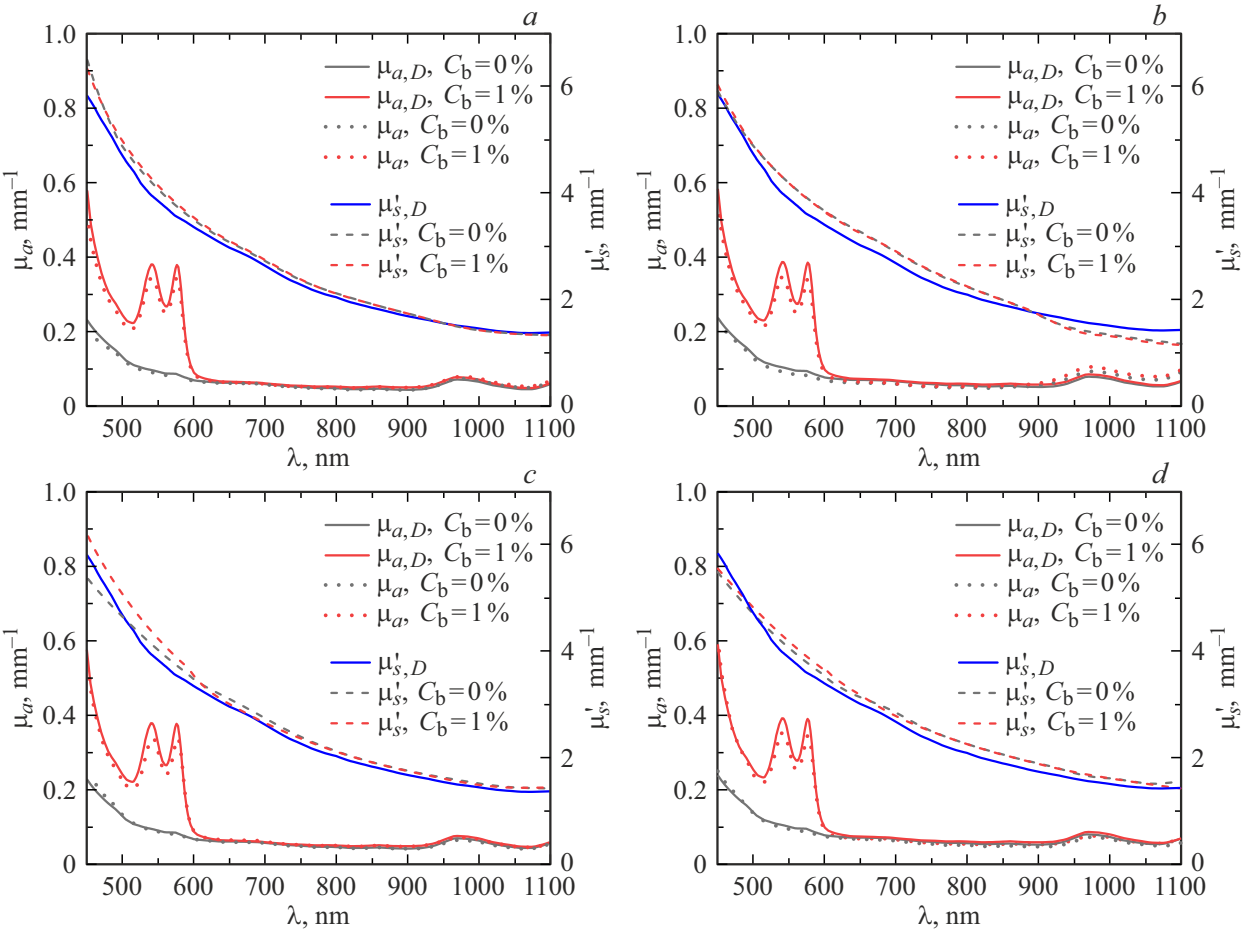

Figure 7. Spectra of absorption coefficient μ_a and transport scattering coefficient μ_s' of a homogeneous dermis with blood-content $C_b = 0$ and $C_b = 1\%$ reconstructed from the ODS signals spectra obtained via modeling by Monte Carlo method for the near (a,b) and distant (c,d) triples of detectors, as well as for the contact (a,c) and contactless (b,d) signals detection. Points correspond to the reconstructed parameters, solid lines — to parameters of homogeneous dermis specified during modeling.

spectrum, the reconstructed values of l_t are close to the values of $l_{t,\mathrm{E}}$, which is due to the predominant propagation of reflected photons in the epidermis due to high absorption. This is most noticeable for the near triplet of detectors (Fig. 8, *b*), for which some part of sensitivity area is located in the epidermis. For the distant triplets of detectors, the underestimation of the reconstructed values l_t is also present (Fig. 8, *d*), but they are not as close to the values $l_{t,\mathrm{E}}$ as in the case of the near-by triplets, since the sensitivity region is shifted deeper in this configuration. With larger values of the wavelength the reconstructed values l_t tend to $l_{t,\mathrm{D}}$. In turn, during contact detection, the near-surface epidermis does not have such a significant effect on the formation of the diffuse field due to the absence of total internal reflection, and for this configuration, it is appropriate to assimilate the effect of epidermis with that of a thin spectral filter.

Fig. 9 illustrates spectra of the primary optical properties $\mu_a(\lambda)$ and $\mu_s'(\lambda)$ reconstructed based on spectra μ_{ef} and l_t of the double-layer medium. From these dependencies, we can see that in case of contact detection of ODS signals and when the signal level is sufficient, the reconstructed optical properties correspond to those of the dermis, and the reconstruction error does not exceed 10–12% for both the near and distant triplets of detectors (Fig. 9, *a* and 9, *c*). However, in case of contactless detection a systematic reconstruction error of up to 30% is observed: the reconstructed values of μ_a turn to be less, and the values μ_s' become greater than the corresponding values of $\mu_{a,\mathrm{D}}$ and $\mu_{s,\mathrm{D}}$ for the homogeneous dermis throughout the studied spectral range (Fig. 9, *b* and 9, *d*). The observed systematic error is slightly lower for the distant detectors triple than for the near triple. This effect is related to the deviation of the reconstructed values l_t from $l_{t,\mathrm{D}}$ shown in Fig. 8, which are then used to calculate the primary optical properties using formulas (3). Previously, a similar effect of overestimating the scattering coefficient and underestimating the absorption coefficient was demonstrated and explained for large values of distances r in [10]. It is worth noting that it also agrees with the results obtained in [28], which have not been explained.

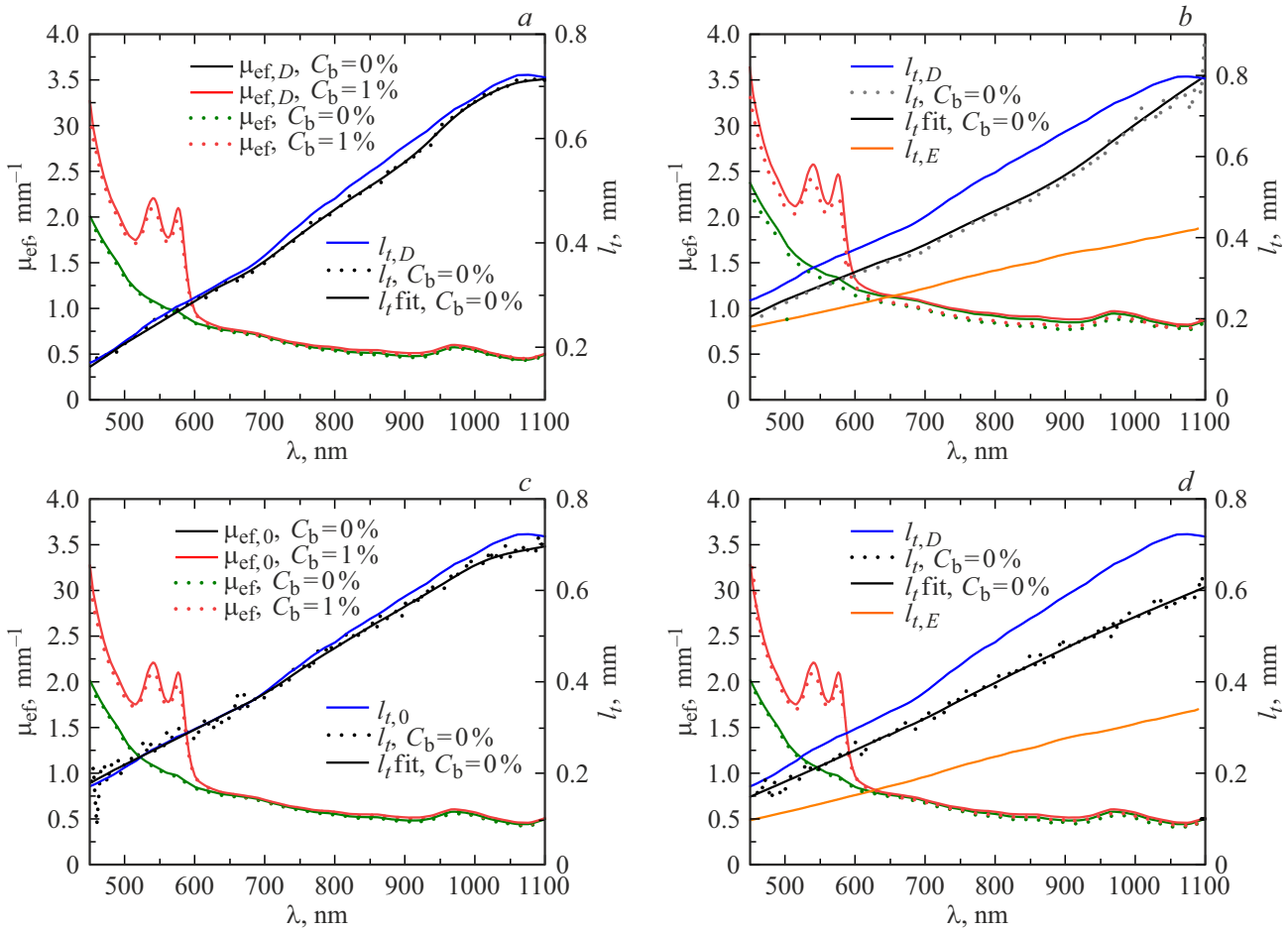

Figure 8. Spectra of diffusive optical characteristics μ_{ef} and l_t of a double-layered skin model containing 100 μm thick epidermis and dermis with blood-content $C_b = 0$ and $C_b = 1\%$, reconstructed from the ODS signals spectra obtained via modeling by Monte Carlo method for the near (*a,b*) and distant (*c,d*) triples of detectors, as well as for the contact (*a,c*) and contactless (*b,d*) signals registration. Points correspond to the reconstructed parameters, solid lines — to dermis parameters set during modeling, as well as to the smoothed reconstructed spectrum l_t (fit).

In conclusion, it should be noted that the present study was conducted accounting for the fixed characteristics of the epidermal layer. However, previous study [10] demonstrated the effect of growing deviation of the reconstructed scattering and absorption spectra from the original dermal spectra with increasing epidermal thickness (i.e., increase of the total melanin content in the near-surface layer) during non-contact detection. A similar effect can be expected when the concentration of melanin in the epidermal layer rises without increasing its thickness.

4. Conclusion

Based on the results of Monte Carlo simulations of optical diffusion spectroscopy signals, the paper outlines the approach to the separate reconstruction of human skin absorption and scattering spectra during contact and non-contact signal detection. A homogeneous skin model, which is a semi-infinite layer of dermis, and a double-layer model, which additionally contains a surface layer of epidermis with a thickness of 100 μm, are considered. An original analytical model of signals recorded by a spatially resolved ODS system with a detector narrow angular pattern is used to reconstruct the optical parameters. The absorption and scattering spectra are reconstructed from two ratios of the ODS signals obtained by numerical Monte Carlo simulation at three source–detector distances. It is demonstrated for the contact detection of ODS signals that when the end of the detecting probe is in close contact with the skin surface, the optical parameters of dermis can be reconstructed with an error of 10% for both a single-layer skin model and in the presence of an epidermal layer. The error is mainly affected by the signal noise, which is lower at shorter source-detector distances. In case of contactless detection, when the skin surface comes into contact with air, the reconstruction error increases. For a homogeneous skin model, significant errors are observed mainly at short source–detector distances and the near-infrared region of the spectrum. In the presence of epidermis, the absorption coefficient is reconstructed with

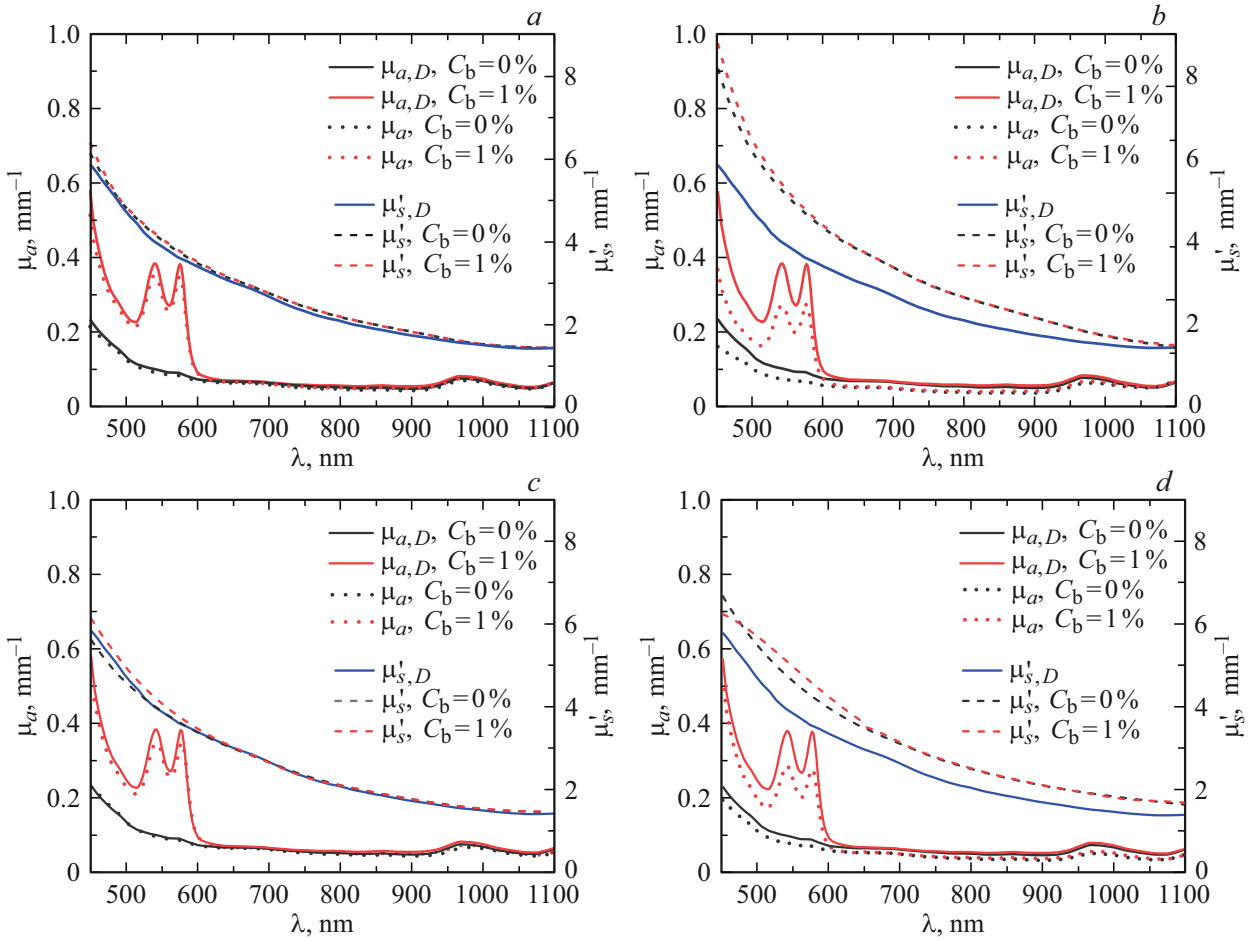

Figure 9. Spectra of absorption coefficient μ_a and transport scattering coefficient μ'_s of a double-layer skin model containing epidermis 100 μm thick and dermis with blood-content $C_b = 0$ and $C_b = 1\%$, reconstructed from the ODS signals spectra obtained via modeling by Monte Carlo method for the near (*a,b*) and distant (*c,d*) triples of detectors, as well as for the contact (*a,c*) and contactless (*b,d*) signals detection. Points correspond to the reconstructed parameters, solid lines — to parameters of homogeneous dermis specified during modeling.

a systematic underestimation, and the scattering coefficient is reconstructed with a systematic overestimation relative to dermis parameters, with an error of about 30%. This discrepancy is caused by the effect of total internal reflection on the formation of diffuse fields in the near-surface layer occupied by the epidermis. It should be noted that when the reconstructed absorption coefficient in the non-contact measurements is systematically underestimated it can lead to an underestimation of the assessed content of various chromophores when they are reconstructed from the absorption spectrum, and also to an error in the estimation of clinically significant skin parameters (such as hemoglobin content). To improve the accuracy of reconstructing the absorption and scattering spectra of the skin subsurface layers in ODS and further determine the clinically significant parameters, it is necessary to measure the spectra in a contact manner with the addition of immersion agents to minimize the effect of the refractive index jump at the skin boundary.

Funding

This study was supported by grant №24-15-00175, from the Russian Science Foundation https://rscf.ru/project/24-15-00175/.

Conflict of interest

The authors declare that they have no conflict of interest.

References

[1] A.J. Moy, J.W. Tunnell. In: *Imaging in Dermatology.* Ed. by M.R. Hamblin, P. Avci, G.K. Gupta (Academic Press, Boston, 2016), p. 203–215.

[2] S.F. Bish, M. Sharma, Y. Wang, N.J. Triesault, J.S. Reichenberg, J.X. Zhang, J.W. Tunnell. Biomed. Opt. Express, **5** (2), 573–586 (2014). DOI: 10.1364/BOE.5.000573

[3] G. Blaney, R. Donaldson, S. Mushtak, H. Nguyen, L. Vignale, C. Fernandez, T. Pham, A. Sassaroli, S. Fantini. Appl. Sci, **11** (4), 1757 (2021). DOI: 10.3390/app11041757
[4] R.H. Wilson, M.A. Mycek. Technol. Cancer Res. Treat., **10** (2), 121–134 (2011). DOI: 10.7785/tcrt.2012.500187
[5] R. Hennessy, S.L. Lim, M.K. Markey, J.W. Tunnell. J. Biomed. Opt., **18** (3), 037003 (2013). DOI: 10.1117/1.JBO.18.3.037003
[6] I. Oshina, J. Spigulis. J. Biomed. Opt., **26** (10), 100901 (2021). DOI: 10.1117/1.JBO.26.10.100901.
[7] M.S. Kleshnin, A.G. Orlova, M.Yu. Kirillin, G.Yu. Golubyatnikov, I.V. Turchin. Quantum Electronics, **47** (4), 355 (2017).
[8] B.C. Wilson. Proc. SPIE, **10306**, 103060H (1990). DOI: 10.1117/12.2283679
[9] T.J. Farrell, M.S. Patterson, B. Wilson. Med. Phys., **19** (4), 879–888 (1992). DOI: 10.1118/1.596777
[10] E. Sergeeva, D. Kurakina, I. Turchin, M. Kirillin. J. Innovative Optical Health Sciences, **17** (5), 2342002 (2024). DOI: 10.1142/S1793545823420026
[11] V. Perekatova, E. Sergeeva, M. Kirillin, A. Khilov, D. Kurakina, I. Turchin. Optics Commun., **579**, 131440 (2025). DOI: 10.1016/j.optcom.2024.131440
[12] Y. Shimojo, T. Nishimura, H. Hazama, T. Ozawa, K. Awazu. J. Biomed. Optics, **25**, 045002 (2020). DOI: 10.1117/1.JBO.25.4.045002
[13] E. Salomatina, B. Jiang, J. Novak, A.N. Yaroslavsky. J. Biomed. Optics, **11**, 064026 (2006). DOI: 10.1117/1.2398928
[14] J.C.J. Wei, G.A. Edwards, D.J. Martin, H. Huang, M.L. Crichton, M.A.F. Kendall. Sci. Rep., **7**, 15885 (2017). DOI: 10.1038/s41598-017-15830-7
[15] J. Sandby-Møller, T. Poulsen, H.C. Wulf. Acta Derm. Venereol., **83** (6), 410–413 (2003). DOI: 10.1080/00015550310015419. PMID: 14690333.
[16] I.L. Shlivko, M.Yu. Kirillin, E.V. Donchenko, D.O. Ellinsky, O.E. Garanina, M.S. Neznakhina, P.D. Agrba, V.A. Kamensky. Skin Research and Technology, **21** (4), 419–425 (2015). DOI: 10.1111/srt.12209 (2015).
[17] V.V. Tuchin. *Optika biologicheskikh tkanei. Metody rasseyaniya sveta v meditsinskoy diagnostike* (FIZMATLIT, Moscow, 2013), in Russian.
[18] A. Kienle, M.S. Patterson. Phys. Med. Biol., **41** (10), 2221–2227 (1996). DOI: 10.1088/0031-9155/41/10/026
[19] T.Y. Tseng, C.Y. Chen, Y.S. Li, K.B. Sung. Biomed. Opt. Express, **2** (4), 901–914 (2011). DOI: 10.1364/BOE.2.000914
[20] D. Kurakina, V. Perekatova, E. Sergeeva, A. Kostyuk, I. Turchin, M. Kirillin. Laser Physics Lett., **19** (3), 035602 (2022). DOI: 10.1088/1612-202X/ac4be8
[21] S.L. Jacques. Phys. Med. Biol., **58** (11), R37-61 (2013).
[22] E. Zherebtsov, V. Dremin, A. Popov, A. Doronin, D. Kurakina, M. Kirillin, I. Meglinski, A. Bykov. Biomedical Optics Express, **10** (7), 3545–3559 (2019). DOI: 10.1364/BOE.10.003545
[23] V. Perekatova, M. Kirillin, S. Nemirova, A. Orlova, A. Kurnikov, A. Khilov, K. Pavlova, V. Kazakov, V. Vildanov, I. Turchin, P. Subochev. Photonics, **9** (7), 482 (2022). DOI: 10.3390/photonics9070482
[24] V. Perekatova, A. Kostyuk, M. Kirillin, E. Sergeeva, D. Kurakina, O. Shemagina, A. Orlova, A. Khilov, I. Turchin. Diagnostics, **13** (3), 457 (2023). DOI: 10.3390/diagnostics13030457
[25] S.L. Jacques. J. Biomedical Optics, **15** (5), 051608 (2010). DOI: 10.1117/1.3494561
[26] A. Isimaru *Rasprostraneniye i rasseyaniye voln v sluchaynoneodnorodnykh sredakh.* (Mir, M., 1981) (in Russian).
[27] R.C. Haskell, L.O. Svaasand, T.T. Tsay, T.C. Feng, M.S. McAdams, B.J. Tromberg. JOSA A, **11** (10), 2727–2741 (1994). DOI: 10.1364/josaa.11.002727
[28] T.J. Farrell, M.S. Patterson, M. Essenpreis. Appl. Opt., **37** (10), 1958–1972 (1998). DOI: 10.1364/ao.37.001958

Translated by J.Savelyeva